Available online at www.sciencedirect.com
SCIENCE DIRECT®
Real-Time Imaging 11 (2005) 99–107
www.elsevier.com/locate/rti

Industrial application for inline material sorting using hyperspectral imaging in the NIR range

Petra Tatzer*, Markus Wolf, Thomas Panner

ARC Seibersdorf research GmbH, Integrated Industrial Inspection, Austria

Abstract

Spectral imaging is becoming increasingly interesting not only for agricultural use but also for industrial applications. Wavelengths in the near infrared (NIR) range, in particular, can be used for materials classification. However, sorting paper according to quality is a very difficult task due to the close similarities between the materials. This work describes the development of a unique industrial inline material sorting system which uses the spectral imaging technique. The main functional parts and the sensor unit are described in detail. Classification methods for cellulose-based materials such as pulp, paper and cardboard will be discussed, as will hardware requirements for the industrial use of spectral imaging solutions, including adjustment and calibration techniques. The description of the software design focuses on the classification speed required.

1. Introduction

Spectral imaging is a new technology combining spectral reflectance measurement and image processing technologies. A hyperspectral imager is similar to a laboratory spectrometer. It produces images over a contiguous range of narrow spectral bands and facilitates the spectroscopic analysis of data [1]. Hyperspectral imaging has now passed the point of scientific curiosity and is currently under active evaluation by researchers in dozens of fields [2]. The near infrared (NIR) range in particular can be successfully used for industrial application for materials classification.

NIR spectroscopy has been used for non-destructive analysis since the first applications for agricultural crop testing in the USA during the 1950s. Today many instrumentation and automation companies are selling dedicated NIR instruments for real-time process monitoring in numerous chemical, food, pulp and paper industry applications. These instruments record sample transmittance or reflectance for a set of wavelengths, and present the end result as, for example, the percentage of moisture for a typical on-line monitoring application. Instrument manufacturers commonly use traditional instrumental techniques, which have limitations when measuring moving, non-homogeneous sample streams in high-speed process applications, as in the paper industry.

Sorting systems for plastics are currently available in different variations, utilizing single-point spectroscopy and the different characteristics of plastics in the SWIR band, as shown in Fig. 1. For sorting paper and cardboard in particular, there will be a growing need for automatic inline sorting units [3,4]. The purer the sorting fraction of waste paper, the more specifically it can be fed back into paper production as a raw material. A decisive quality criterion for waste paper is based on the observation of whether it is composed of bleached (chiefly paper) or unbleached (chiefly cardboard) fibres. Since waste paper is not rebleached when it is fed back into paper production as a raw material, only waste paper with fibres that have already been bleached can be used for the production of white or very light coloured

*Corresponding author. Tel.: +43 50550 2705; fax: +43 50550 2724.
E-mail address: petra.tatzer@arcs.ac.at (P. Tatzer).
URLs: http://www.arcs.ac.at/W/WPQ, http://www.machine-vision.at.

1077-2014/$ - see front matter © 2005 Elsevier Ltd. All rights reserved.
doi:10.1016/j.rti.2005.04.003

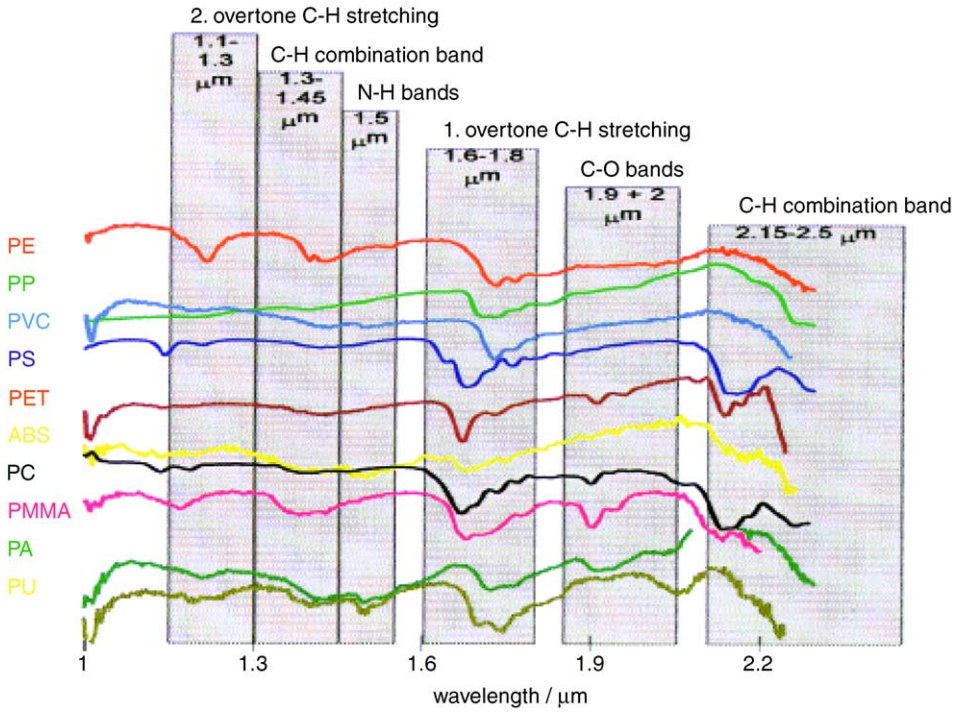

Fig. 1. Absorption spectra of different plastics.

paper. Furthermore, the stock of long pulp fibres in recycling is crucial for the consistent quality of the end product. Separating short-fibre cardboard materials from long-fibre papers is becoming increasingly important in paper processing.

In this paper, the prototype of a paper sorting system is presented which uses the hyperspectral imaging technique for materials identification. Classification methods for cellulose-based materials such as pulp, paper and cardboard will be discussed, as will hardware requirements for the industrial use of hyperspectral imaging solutions, including adjustment and calibration techniques. The description of the software design focuses on the classification speed required.

The paper is organized as follows: Section 2 gives a general system overview, including sorting and the sensor unit as well as hardware adjustment and calibration methods for the sensor unit. Data preprocessing and normalization, feature reduction for spectra analysis and classification methods are described in Section 3. Section 4 deals with the results of the experiment. With regard to real-time aspects, the software concept is shown in Section 5. Finally, Section 6 concludes our work.

2. General system overview

The system described (Fig. 2) is an inline sorting unit for materials classification designed for the inspection of recovered paper. The system supports two-way sorting and has been developed for sorting paper and cardboard from household collections to achieve pure paper fractions.

The main conveyor belt moves the pieces of material to be classified across the monitoring station with a typical velocity of 2 m/s. The sensor unit acquires spectral data continuously at fixed intervals. The width of the conveyor belt is divided into 288 sections and an individual spectrum is acquired for each of these sections. After data preprocessing and reduction, a classification algorithm is applied to the spectral data to perform the materials classification. The results of the classification, which form an array with 288 entries, are transferred from the PC that performs the material analysis to the PC that controls the whole facility via an Ethernet connection.

A beam carrying an array of nozzles is mounted at the end of the main conveyor belt. Each nozzle can be triggered individually for a time frame corresponding to the extent of the object. Pieces to be sorted out of the stream of material are ejected by compressed air and transferred to a second conveyor belt. The rest of the material drops onto a third conveyor belt mounted below the gap between the main and second conveyor belts.

2.1. Sensor unit

The working principle of the sensor unit is the NIR reflectance measurement within the spectral range from 900 to 1700 nm. The sensor unit consists of the following

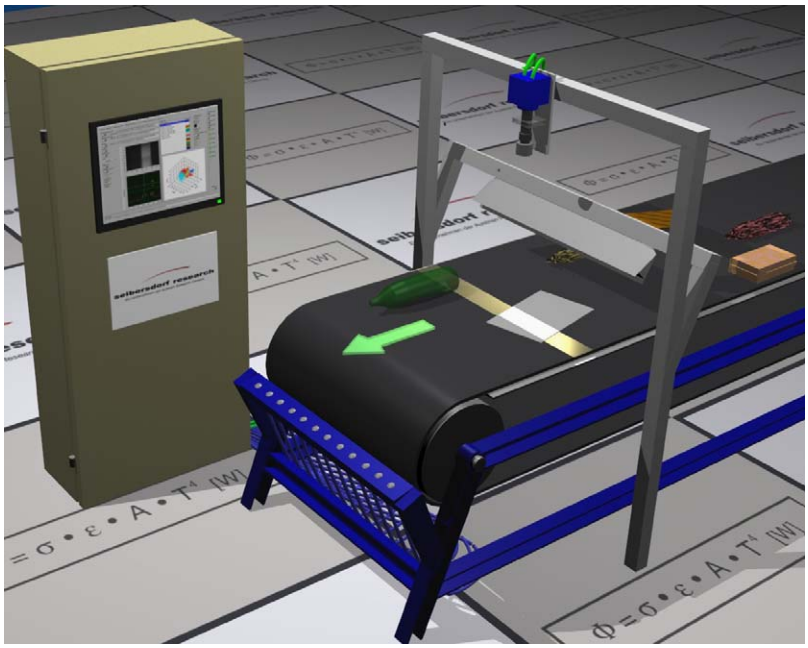

Fig. 2. Functional principle of the sorting unit.

hardware components: camera, spectrograph and illuminator.

The camera system functions using an InGaAs sensor (XEVA-USB-FPA-1.7-320-TE1, XenICs, Belgium) with spectral sensitivity from 900 to 1700 nm and a nominal resolution of 320 × 256 pixels. An NIR-optimized lens is mounted in front of the spectrograph, governing the resolution and the field of view. The frame rate is up to 100 full frames per second. The system generates the data with 12-bits per sample representation. The generated data set is transferred to the processing system using a high-speed serial link with a maximum speed of >400 Mbit/s. Prerequisites for obtaining properly calibrated data include constant sensor temperature, since noise and cutoff wavelength depend on the sensor temperature, and full detection of defective pixels (not connected, non-linear or other non-uniformities), including influenced neighbour pixels. Up to 2% of the sensor pixels are defective.

An imaging spectrograph (ImSpector N17, Specim Ltd., Finland) with a spectral range from 900 to 1700 nm and a spectral resolution of 13 nm is used. Light reflected by the object to be classified is projected onto the entrance slit of the imaging spectrograph. The ImSpector contains a prism-grating-prism arrangement which analyses the incoming light and projects the spectral image onto the camera chip [5]. There was no need to use an order blocking filter to suppress higher-order signals since the wavelength ratio λ_2/λ_1 is $\leqslant 2$. In our case λ_2 is 1700 nm and λ_1 is 900 nm; it thus follows that $\lambda_2/\lambda_1 = 1.88$.

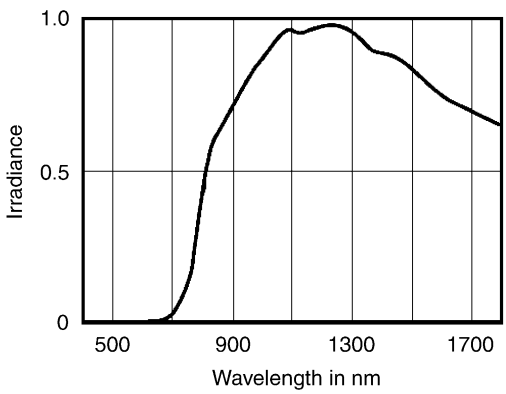

Fig. 3. Spectral emission curve of the illumination used.

To achieve sufficient light intensity for reflectance measurement in the NIR range, the samples have to be illuminated within the proper spectral range and with sufficient intensity. The illuminator therefore consists of eight halogen lamps with a radiation intensity of $>70\%$ in the range of 900–1700 nm (see Fig. 3). As can be seen in Fig. 2, the material on the conveyor belt is illuminated at an angle of 70°.

2.2. Adjustment and calibration

When using a spectrograph, image distortions can be caused by imperfections of the grating, the prism and the lens system. Adjustment and calibration of the camera and spectrograph are therefore necessary. The sensor unit classifies passing material. The more

accurate the per pixel result calculated by the sensor unit, the better the outcome of the whole sorting process. With this focus in mind, the following sections describe methods for adjustment, calibration, normalization, feature reduction and classification.

2.2.1. Adjusting the camera and spectrograph

The camera and spectrograph must be carefully adjusted so that the spectral dimension is precisely projected in a vertical direction onto the sensor chip. This adjustment is made using the peaks within the spectrum of the wavelength calibration lamp. Within the camera image these peaks occur not as sharp lines but as relatively wide lines which are often parabolically bent by the spectrograph itself. Due to the presence of these impairments, the axis of the spectrograph and sensor array cannot be aligned by simple visual adjustment when the rotational difference is less than 1 pixel.

The position of each maximum in each row must be calculated using subpixeling. As described in [6] the procedure is composed of the following steps:

(1) Estimate the spectral centre position of each peak for every spatial pixel across the spatial axis.
(2) Fit a second-order polynomial through the estimated peak centres.
(3) Estimate the spectral peak positions for the first and last spatial pixel columns using the second-order polynomial.
(4) Estimate the difference between the two peak positions.
(5) Rotate the camera until the difference is zero.

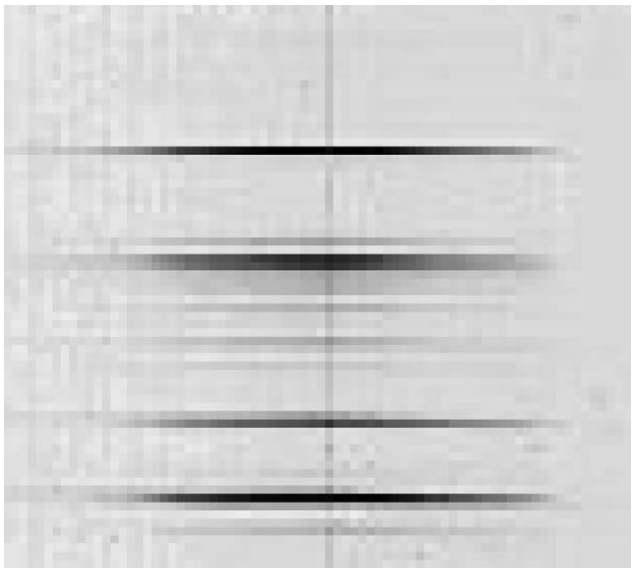

Fig. 4. Captured camera image of wavelength calibration lamp.

2.2.2. Spectral calibration

Spectral or wavelength calibration is required for assignment between pixel position and wavelength within each column. A gas extinction lamp with spectral bands covering the entire spectral range is used for this assignment.

Fig. 4 shows the inverted raw image data captured by a hyperspectral imaging sensor unit produced by a mercury–argon lamp. The vertical direction of the image holds the spectral information, while the horizontal direction corresponds to the spatial information. As can be seen, four main spectral peaks appear as dark horizontal lines and there are several additional wavelength peaks. All lines correspond to the measured spectral intensity of the wavelength calibration lamp shown in Fig. 5. The four main peaks, which can be seen as black lines in the image in Fig. 4, correspond to the

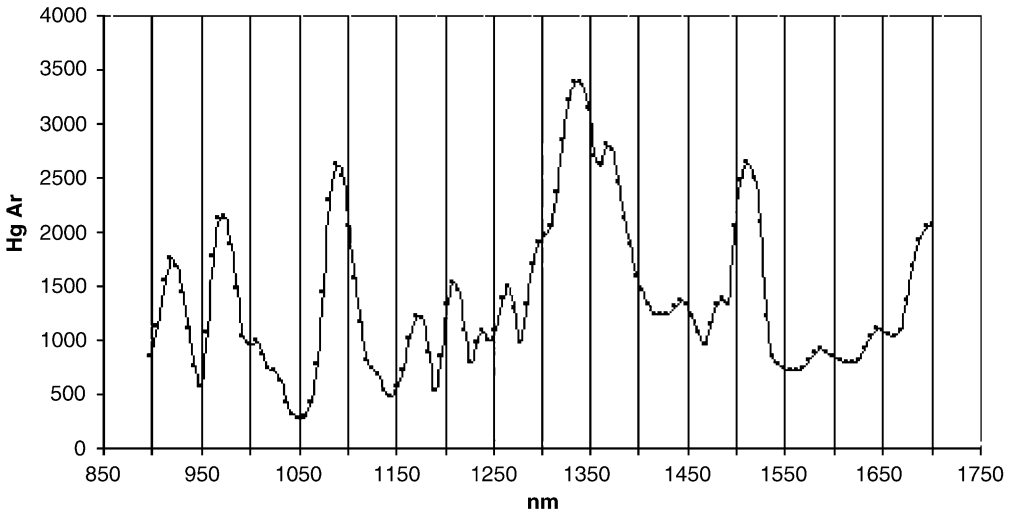

Fig. 5. Measured spectral intensity of mercury–argon wavelength calibration lamp.

wavelengths 975 nm (bottom line), 1090, 1340 and 1510 nm (top line), respectively.

3. Preprocessing, spectra analysis and classification

Before applying any classification to the data, it is necessary to perform some preprocessing such as replacement of the poorly connected pixels and correction of the dark current as well as the dynamic range.

NIR cameras have the problem of defective pixels that always appear dark or always appear bright. Bright pixels are always saturated due to localized defects in the InGaAs material or a short circuit from the InGaAs to the readout multiplexer. Dark pixels are open pixels which have no response to light and are caused by a bad connection from the InGaAs element to the CMOS readout [7]. This necessitates the use of a multistage detection procedure. The detection process starts with the recording of one dark and one white image. The dark image, which represents the sensor noise, is captured using a dark cover in front of the optics. The white image is captured by looking at the white standard, which is a material with known spectral reflection values over the full spectral range. Bad pixels are detected as bright pixels within the dark image and black pixels within the white image. Finally, the process is completed by replacing the marked pixels with the nearest non-defective pixel in the vertical direction.

To measure reflectance, both the incident intensity and the scattered reflectance should be measured in absolute units. This is very often impractical, so a reference material of known spectral properties is used to normalize the data. Furthermore, the dark current contributes to the signal coming from the sensors, and this should be subtracted from the data. The reflectance is therefore computed as

$$I = \frac{I_s - I_d}{I_w - I_d}, \tag{1}$$

where I_s is the measured sample data, I_d is the dark current image and I_w is the white image captured from reference material.

3.1. Analysis of spectra

The main advantage of hyperspectral images is the large amount of information that can be obtained as a result of the large number of continuous spectral bands. In order to design a stable and reliable classification algorithm capable of coping with vast amounts of data in an inline application, standard chemometric methods are used for data reduction.

Chemometrics can be defined as the chemical discipline that uses mathematical, statistical and other methods employing formal logic to design or select optimal measurement procedures and experiments, and to provide maximum chemical information by analyzing chemical data [8,9].

Our aim is to find an optimal subspace for classification by testing two feature reduction methods. The two methods considered are principal components analysis (PCA) and linear discriminant analysis (LDA).

PCA is used to reduce data and obtain as much information as possible about the characteristics of the samples by transforming the original multidimensional data space into a space with lower dimensions [10]. The idea of PCA is to approximate the original matrix D using the product of two smaller matrices—the score and the loading matrices—according to:

$$D = TL^T, \tag{2}$$

where D is the original data matrix consisting of n rows (objects) and p columns (features), T the matrix of scores with n rows and d columns (number of principal components); L the loading matrix with d columns and p rows; and the symbol T denotes the matrix transpose.

Like PCA, LDA is a method that transforms the data space. PCA looks for the direction with most scattering, independent of different classes. The objective of LDA is to perform dimensionality reduction while preserving the class discriminatory information as much as possible.

As described by Naes et al. [10], the LDA procedure starts with the calculation of two matrices. The within-scatter matrix, which is defined as

$$S_w = \sum_{i=1}^{C} \sum_{j=1}^{N_i} (x_{ij} - \mu_i)(x_{ij} - \mu_i)^T, \tag{3}$$

describes the scatter within one class, whereas the inter-scatter matrix, defined as

$$S_B = \sum_{i=1}^{C} (\mu_i - \mu)(\mu_i - \mu)^T N_i, \tag{4}$$

describes the scatter between classes. In both the equations above, x represents a spectrum in the original multidimensional data space, μ_i is the centre of a specific class, N_i is the number of spectra for a specific class, x_{ij} is the jth spectrum in ith class, C is the number of classes and μ is the centre of the whole data set.

The next step for computing the LDA is to maximise the ratio between S_B and S_W, which corresponds to calculating the eigenvectors and eigenvalues of the matrix $S_W^{-1} S_B$. We thereby obtain a set of vectors defining the directions which discriminates as much as possible between all groups [10].

3.2. Classification

In this section the *k-nearest neighbour* (k-NN) classification algorithm, which was used to perform

the classification task, will be described. The k-NN method introduced by Fix and Hodges in 1951 is a simple non-parametric but supervised classification technique [8] which has been shown to be very effective in statistical pattern classification applications.

The principle of k-NN is that pixels that are close to each other in the feature space are likely to belong to the same class. Thus k-NN uses a distance measure $d(x, y)$ to calculate the closeness between pixel vectors. To classify an unknown object we calculate its distance from all the objects in the training set. The minimum distance is selected and the object is assigned to the corresponding class. The number of neighbouring objects is typically chosen to be 1 or 3. Very flexible separation boundaries are obtained with the k-NN method [8]. For a detailed description of k-NN see [8,10].

4. Results and discussion

The basis of our work is composed of hyperspectral images taken from 200 carefully selected samples: 100 samples of paper and 100 samples of cardboard. All the samples selected have a minimum size of 200×300 mm and can be clearly identified as either raw cardboard, coloured cardboard, newspaper or printer paper. The samples have no stickers or labels and no extensive black printing. Every 12-bit hyperspectral image file contains one line of the sample with a spatial resolution of 5 mm per pixel and 180 pixels for the wavelength in the spectral range from 900 to 1700 nm. On the basis of this data, we attempted to find a classification model to distinguish between paper and cardboard. Although the spectra of materials such as cardboard and newspaper are very similar, it is possible to distinguish between them using the methods described above. Fig. 6 shows typical spectra of cardboard and paper.

Due to the so-called multicollinearity problem, the calculation of the LDA could be unstable. Therefore a PCA is performed on the data set first to reduce dimensionality. The scores from the PCA represent the input data for the subsequent LDA calculation. Fig. 7 shows the differences between a simple PCA and a combination of PCA and LDA. The two methods were applied to the same simplified data set, which consists of reflectance spectra of coated paper, brown cardboard and grey newspaper. However, the aim of PCA is not to separate the classes; it is possible to distinguish between coated paper (blue) and the other two classes. Brown cardboard is ingrained in grey newspaper, which prevents reliable classification. The combination of PCA and LDA allows all three classes to be separated. Fig. 8 compares the results of a simple PCA and a combined PCA/LDA based on the same data set consisting of cardboard (red), newspaper (blue) and white office paper (green). Each class contains data from several individual samples, so that the classification model created is representative of the specific characteristics of the classes to be separated. While the clouds of newspaper and cardboard overlap in the PCA model, they could be separated almost completely in the combined PCA/LDA model.

To validate a classification model and to compare different models, an independent data set acquired on predefined samples is used. The samples are divided into subgroups according to the classes contained in the classification model. The data from each sample is classified and evaluated separately by counting the number of spectra assigned to each class and calculating the misclassification percentages. To obtain an expressive figure, the mean of the percentages assigned to the

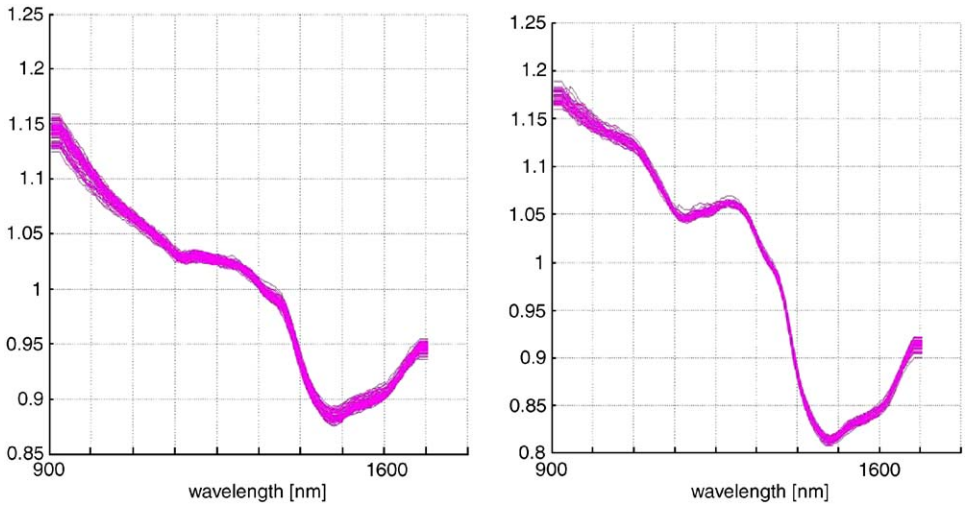

Fig. 6. Normalized reflectance spectra of individual samples; spectra of a white cardboard sample (left) and a white paper sample (right).

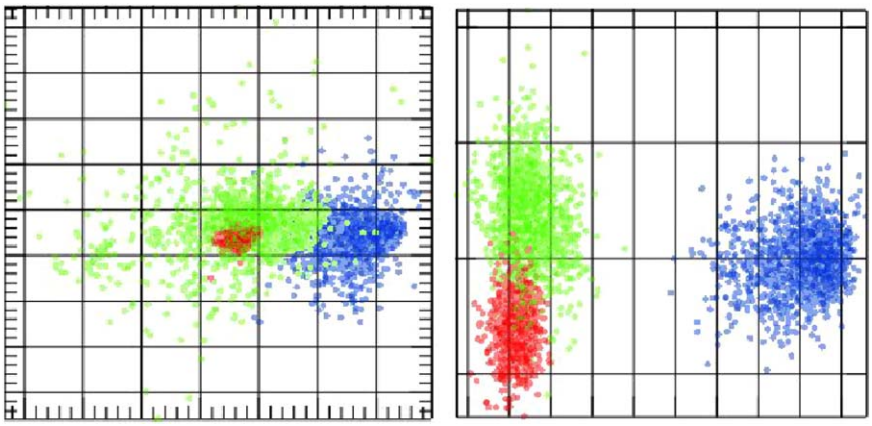

Fig. 7. Training set composed of three different materials: white paper (blue), cardboard (red) and newspaper (green); PCA model (left) and LDA model (right).

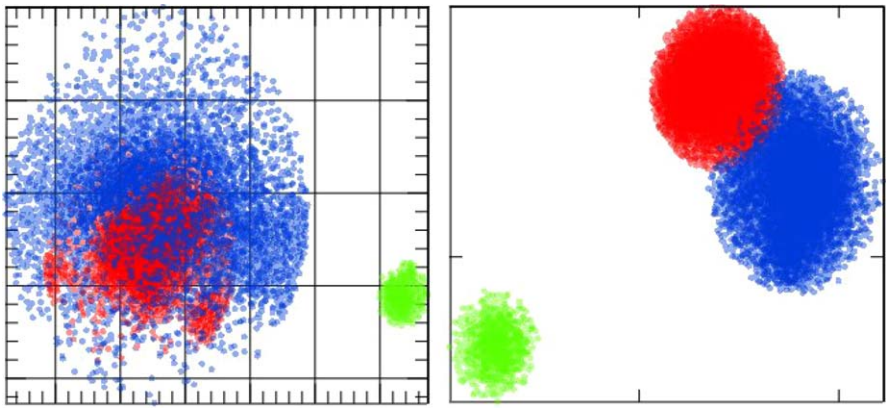

Fig. 8. Training set composed of three different materials: white paper (green), cardboard (red) and newspaper (blue) with PCA (left) vs. PCA/LDA (right).

correct class of the classification model over all members of each sample subgroup is calculated. Table 1 shows the mean percentages of the results of all subgroups.

The performance of the sensor system described in this paper is measured by per-pixel validation, as explained above. Of course, other criteria have to be applied to the whole sorting system. The most common method in the recycling industry is to use a large number of samples and to calculate the ratio of the weights of the two outputs (ejected/not ejected) compared to the weight of the input material. Two main figures express the error rate of the erroneously accepted and erroneously rejected material for a two-way sorting system of this type. It is not possible to precisely predict the overall performance of the sorting system based on the per-pixel results, due to additional error sources such as overlapping objects on the conveyor belt and errors caused by the effectors. The only reliable way of investigating the overall performance of the sorting system is to set up the whole system, run it and physically count the misclassified objects (pieces of paper).

Table 1
Best classification results

	PCA	PCA/LDA
Raw cardboard	52%	93%
Coloured cardboard	33%	81%
Newspaper	55%	95%
Printer paper	70%	91%

5. Software concept

In order to improve the performance of the entire spectral imaging system, a multithreaded application

was set up with an open design for simple connection of additional modules. Creating multiple threads for the application leads to improved performance, starting with operating systems supporting multithreading and a single processor with multithreading support (e.g. Intel's Hyper-Threading Technology). Due to more efficient use of the processor's resources, Hyper-Threading leads to performance enhancements of up to 30% [11]. A key factor for the efficiency of Hyper-Threading is the amount of time for which the "simultaneous" running threads are running at full speed, since there is only one physical processor which is presented to the software as two complete CPUs. Full advantage of the multithreaded approach can be taken using a multiple processor machine where symmetrical multiprocessing (SMP) balances the processing load on different CPUs.

The software needs to fulfill functionality and speed requirements. Therefore the three main tasks of image acquisition (obtaining the image from the camera), data processing (preprocessing, data reduction and classification) and communication had to be designed and implemented with the objective of a maximum delay of less than 16.6 ms between an image being requested and the classification results being transferred. This means that the sorting system runs at a scan rate of 60 Hz.

Our first approach was straightforward, linking the three tasks together (Fig. 9). This results in a total processing time of 20 ms, where the time for grabbing is about 10 ms. Testing with a simple "grab and wait for ready" loop showed that the CPU load increased by less than 15%. This means that for most of the task, the CPU is waiting for image transfer to be completed.

Due to the low CPU load for requesting and receiving the image data from the camera, the task of grabbing images is performed by an image server that handles the complete image grab and preprocessing. The preprocessed data is passed on to the processing thread using a ring buffer created in a shared memory space. If the processing thread is ready to perform the next classification cycle, it accesses the latest image available in the shared memory. The results are placed in the second ring buffer, which holds the classification results. Both the communication module that transmits the results to PLC and the data logging module have access to these results (Fig. 10).

Using this concept reduces the time for one cycle (grab-process-communicate) from 20 to 15 ms without using a dual processor system. Using a dual processor system gives an additional speed boost without changing

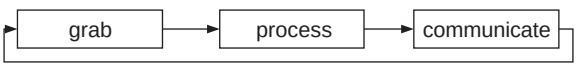

Fig. 9. Block diagram of single-threaded approach.

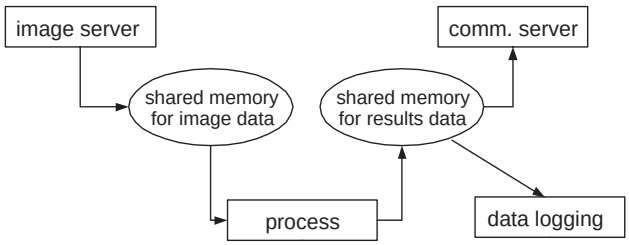

Fig. 10. Multithreaded approach.

the code by performing the grab process on one CPU and the image processing on the other CPU.

The first approach for the k-NN classification was straightforward: calculate and store the Euclidean distance from the unknown test point to all training data points, sort the array, calculate the n points with the smallest distance, find the class label of the points and evaluate the "k out of n" rule.

Estimating the CPU load showed that calculating the distance between two points $(x - x_t)^2 + (x - y_t)^2 + (z - z_t)^2$ requires 8 FLOPS and at least 7 transfers per point. The search for the minimum distance requires 1 FLOP and 2 transfers. Assuming that 100,000 points of training data are used, all data is stored as double (8 bytes per value) and k-NN is used (3 out of 5), this gives 800,000 FLOPS for the distance calculation and 500,000 FLOPS for the five nearest neighbours. The theoretical floating-peak performance of an Intel Pentium 4 running at 3 GHz is approximately 6 GigaFLOPS, which gives a calculated time consumption of 217 μs for the calculation of the five nearest neighbours. Additional time is required for the memory transfers ($7 \times 8 \times 100,000 + 2 \times 5 \times 100,000 = 6.3$ MB per classification point). Having an average memory performance for move operations of 3200 MB/s gives a time of approximately 2 ms for the transfers. This means that the total time consumption per classification point is $0.217\,\text{ms} + 2\,\text{ms} = 2.217\,\text{ms}$. The time for full image classification (288 points) is at least 638.5 ms on a 3 GHz P4. This simple estimation ignores overhead for the loops, conditional copy of the minimum value, calling overheads and hardware interrupts.

In order to go real time, the calculation work was removed from the inline part. It was decided to generate a lookup table for the complete target space. This discrete space representation (DSR) is calculated offline using the k-NN classification and is saved as a binary file. When performing real-time classification, each PCA/LDA-converted sample point is transformed into a discrete coordinate dividing the component value by the DSR resolution. These discrete coordinates together form an offset into the lookup table where the classification result can be read. This approach achieves a performance of inline classification speed for 288 points of 2 ms, independent of the size of the training

data. With this solution, a scan rate of 60 Hz for material classification is achieved.

6. Conclusion

We have shown that hyperspectral imaging in the near infrared range between 900 and 1700 nm is a method of inline material classification not only for polymers but also for cellulose-based materials such as pulp, paper and cardboard. The best classification performance is currently obtained using a combination of PCA and LDA for feature reduction combined with a carefully selected set of training data and a k-NN classification algorithm. In addition, the real-time aspects of inline classification can be realized using a precalculated discrete space representation.

Acknowledgments

This work was partly supported by the FFF project OIDIPUS, under the grant number 809021-KA/SA. We gratefully acknowledge the reviewers' valuable comments and suggestions.

References

[1] Johnson BD. Spectral imaging finds a place on the farm. Photonics Spectra Magazine, January 2002, Laurin Publishing, 2002.
[2] Directions in Environmental Spectroscopy, Spectroscopy Showcase Magazine, March 1999.
[3] Putz H-J, Göttsching L. Altpapier – Ist sein Einsatz noch zu steigern? Das Papier 2001 – T189.
[4] Spotlight on paper collection and recycling: challenges and opportunities of the future. Brussels 28th October 2002.
[5] Hyvarinen T, Herrala E, Dall'Ava A. Direct sight imaging spectrograph: a unique add-on component brings spectral imaging to industrial applications. SPIE 1998, symposium on electronic imaging in conference 3302, 1998.
[6] Rasmus NJ. The VTTVIS line imaging spectrometer—principles, error, sources, and calibration. Denmark: Pitney Bowes Management Services; 2002.
[7] Application note: what are all these white spots? Sensors unlimited, Doc. No. 4110-0031 Rev. B, 2004.
[8] Otto M. Chemometrics, statistics and computer application in analytical chemistry. New York: Wiley-VCH; 1999.
[9] Einax JW, Zwanziger HW, Geiß S. Chemometrics in environmental analysis. Weinheim: VCH; 1997.
[10] Tormod N, Thomas I, Tom F, Tony D. Multivariate calibration and classification. NIR Publications; 2002.
[11] White paper on hyper-threading technology architecture and microarchitecture. Intel Technology Journal 2002; Q1.